Vol 17 No 3, March 2008
1674-1056/2008/17(03)/1130-05
Chinese Physics B
© 2008 Chin. Phys. Soc.
and IOP Publishing Ltd

Angular dependence of coercivity of grains in nanocrystalline permanent magnets*

Gong Yi-Min(龚依民)[a], Lan Zhi-Huan(蓝志环)[a], Yan Yu(闫 羽)[a],
Du Xiao-Bo(杜晓波)[a]†, Wang Wen-Quan(王文全)[a], Wang Xue-Feng(王学凤)[a],
Su Feng(苏 峰)[a], Lu Lei(卢 磊)[a], Zhang Zhi-Sheng(张之胜)[a],
Jin Han-Min(金汉民)[a], and Wen Ge-Hui(温戈辉)[b]

[a] *Department of Physics, Jilin University, Changchun* 130023, *China*

[b] *State Key Laboratory of Superhard Material, Jilin University, Changchun* 130023, *China*

(Received 3 April 2007; revised manuscript received 18 July 2007)

In this paper magnetization remanence curves were studied for nanocrystalline $Pr_8Fe_{87}B_5$, $Pr_{12}Fe_{82}B_6$ and $Pr_{15}Fe_{77}B_8$. Initially the sample was at remanence following saturation along z-axis. After rotating the magnet by $5n$ degrees (n=0, 1, ..., 18) a field H was applied along z-axis and then decreased to zero, and the remanence J_r^n was measured as a function of H. The curves were compared with those calculated based on the nucleation of reverse domain model and domain wall pinning model. The latter model succeeds in simulation much better than the former, and it is concluded that the magnetization reversal is dominated by domain wall pinning for all the samples. The nucleation mechanism contribution, while remains small, increases with the increase of Pr content.

Keywords: nanocrystalline, permanent magnets, magnetization curves, computer simulation
PACC: 7550V, 7560, 7540B, 7540M

1. Introduction

Coercivity is one of the most important properties of permanent magnets, and the mechanism has been explored for many years. If the demagnetization proceeds by coherent magnetization rotation, the intrinsic coercivity ${}_{\rm i}H_{\rm c}$ equals to the anisotropy field $H_{\rm A}$ for a uniaxial magnet. In real magnets, the demagnetization processes are characterized by the nucleation and growth of the reverse domain and the pinning of the domain wall, the values of ${}_{\rm i}H_{\rm c}$ are around $(1/10–1/3)H_{\rm A}$.[1,2] The coercivity, in general, has been explained either by the nucleation model or pinning model. The former or latter model would be proper if the critical field of the nucleation and growth is larger or smaller than that of wall pinning.[3,4] The mechanisms could be distinguished from analysis of experimental data of initial susceptibility, ${}_{\rm i}H_{\rm c}$ as a function of maximum magnetizing field, temperature or angle between the applied field and the alignment direction and etc.[5–8] It is generally accepted that the mechanism for sintered $SmCo_5$ and Nd–Fe–B magnets is the nucleation and that of sintered $Sm_2(CoFeCuZr)_{17}$ the pinning. As for nanocrystalline magnets no consistent conclusion has been reached yet.[7–12]

${}_{\rm i}H_{\rm c}$ of aligned magnet as a function of the angle between the alignment (easy axis) and field directions θ (>0) is given by the nucleation model as[9,13]

$$ {}_{\rm i}H_{\rm c}^n(\theta) = {}_{\rm i}H_{\rm c}^n(0)[1+2K_2\tan^{\frac{2}{3}}\theta/K_1(1+\tan^{\frac{2}{3}}\theta)]/(\cos^{\frac{2}{3}}\theta+\sin^{\frac{2}{3}}\theta)^{\frac{3}{2}}, \quad (1) $$

where K_1 and K_2 are the anisotropy constants, and by the pinning model as[14]

$$ {}_{\rm i}H_{\rm c}^{\rm p}(\theta) = {}_{\rm i}H_{\rm c}^{\rm p}(0)/\cos\theta. \quad (2) $$

The two relations are quite different: with increase of θ from 0 to 90°, ${}_{\rm i}H_{\rm c}^n(\theta)/{}_{\rm i}H_{\rm c}^n(0)$ decreases slightly from 1 and then increases slightly to $1+2K_2/K_1$. ${}_{\rm i}H_{\rm c}^n(\theta)/{}_{\rm i}H_{\rm c}^n(0)$, in contrast, increases monotonically to infinity.

This work proposes an experimental procedure to measure the angular dependence of ${}_{\rm i}H_{\rm c}$ for the grains

*Project supported by Department of Science and Technology of Jilin Province, China.
†E-mail: duxb@mail.jlu.edu.cn

of isotropic nanocrystalline magnet. The experimental results are compared with the calculations using Eqs.(1) and (2). The experimental results of nanocrystalline Pr–Fe–B magnets coincide with the pinning model rather than nucleation model. Correlative work has been reported.[15,16]

2. Samples and experimental methods

$Pr_8Fe_{87}B_5$, $Pr_{12}Fe_{82}B_6$ and $Pr_{15}Fe_{77}B_8$ nanocrystalline ribbons were prepared by arc melting pure Pr and Fe metals (≥99.9%) and Fe–B alloy and melt-spinning the ingots in pure argon atmosphere at optimal wheel speeds of around 20m/s. The phases of the samples were analysed by x-ray diffraction with Cu Kα radiation (Rigaku Rint). Magnetic measurements were performed by using a vibrating sample magnetometer (Lake Shore 7410) at room temperature. The field was applied parallel to the surface of the square ribbon sample. The samples consist of $Pr_2Fe_{14}B$ and additional phases. The additional phases and the values of the remanence J_r, coercivity ${}_iH_c$ and maximum energy product $(BH)_{max}$ are listed in Table 1.

Table 1. Additional phases and magnetic properties of the samples.

composition	additional phases	J_r/T	${}_iH_c$/(kA/m)	$(BH)_{max}$/(kJ/m^3)
$Pr_8Fe_{87}B_5$	Fe	1.19	416	140
$Pr_{12}Fe_{82}B_6$	–	0.91	904	143
$Pr_{15}Fe_{77}B_8$	Pr-rich and +B-rich	0.78	1360	112

3. Experimental procedure and results

Initially the magnet is set at remanence J_r after saturation along z-axis. The magnet is rotated around x-axis by an angle $\theta_n \equiv 5n$ (n=0, 1, 2, ..., 18) degrees, and a field H is applied along z-axis and then decreased to zero and the remanence is measured. The remanence depends on both n and H, and the magnetization remanence curve (MRC) $J_r^n(H)$ is measured for each n.

Suppose the inter-grain interactions can be neglected. At the initial state of J_r the magnetization vector directions of the grains are along the easy-axis directions and are distributed homogeneously within $z > 0$ hemisphere. The hemisphere is evenly divided into 2×18 lamellas perpendicular to the yz plane. The top angle of the thin fan-shape section of each lamella is 5° and the angle between z-axis and the average easy axis direction of lamella m (< 18) and 36–m is θ'_m =92.5–5m degrees anti-clockwise and clockwise, respectively (Fig.1(a)). The magnetization process during the measurement of $J_r^0(H)$ is reversible and hence $J_r^0(H) = J_r = \sum_m^{1,2,\ldots,18} 2j_r^m(H) = \sum_m^{1,2,\ldots,18} 2j_r^m$, where $j_r^m = j_r^{36-m}$ is the contribution of initial state lamella m.

When the magnet is rotated by θ_n lamella 1 becomes a lamella which is equivalent to initial state lamella 36–n. The magnetization vector distribution is opposite to the latter, the contribution of lamella 1 to new remanence is $-j_r^n$. During following magnetization along z-axis irreversible magnetization processes occur in the lamella in a critical field range and the magnetic vector distribution at new remanence becomes that of initial state lamella 36–n if H is larger than the critical fields of the lamella (Fig.1(b)). The field dependence of the contribution of lamella 1 being denoted by $j_r^n(H) j_r^n(H) - j_r^n$ is obtained from the experimental MRC as

$$j_r^n(H) - j_r^n = J_r^n(H) - J_r^{n-1}(H). \qquad (3)$$

The field $h(\theta'_n)$ corresponding to the maximum of $\mathrm{d}j_r^n(H)/\mathrm{d}H$ represents the coercivity of the grains of initial state lamellas n and 36–n.

Figure 2(a) to 2(c) show the experimental results of $J_r^n(H)/J_r$. The $h(\theta')/h(0)$ curves will be presented in the next section.

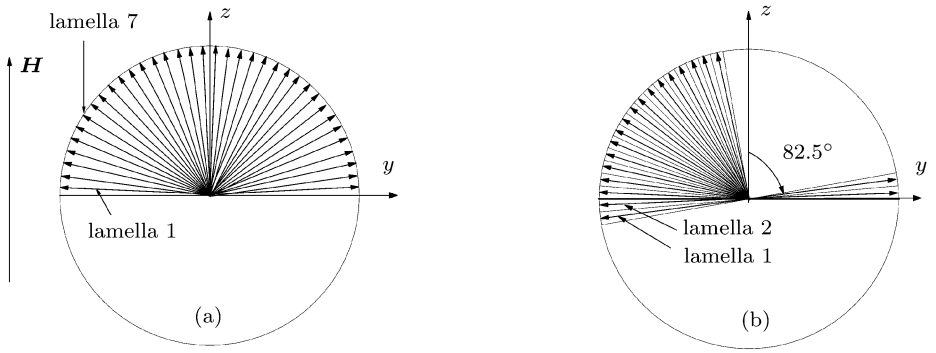


Fig.1. Distribution of magnetization vectors at initial remanence state (a), and that of the left half hemisphere after the magnet is rotated by 10° (left in (b)). The magnetization vector directions of lamellas in the negative hemisphere reverse after magnetized along the z-axis by a large enough field (right in (b)).

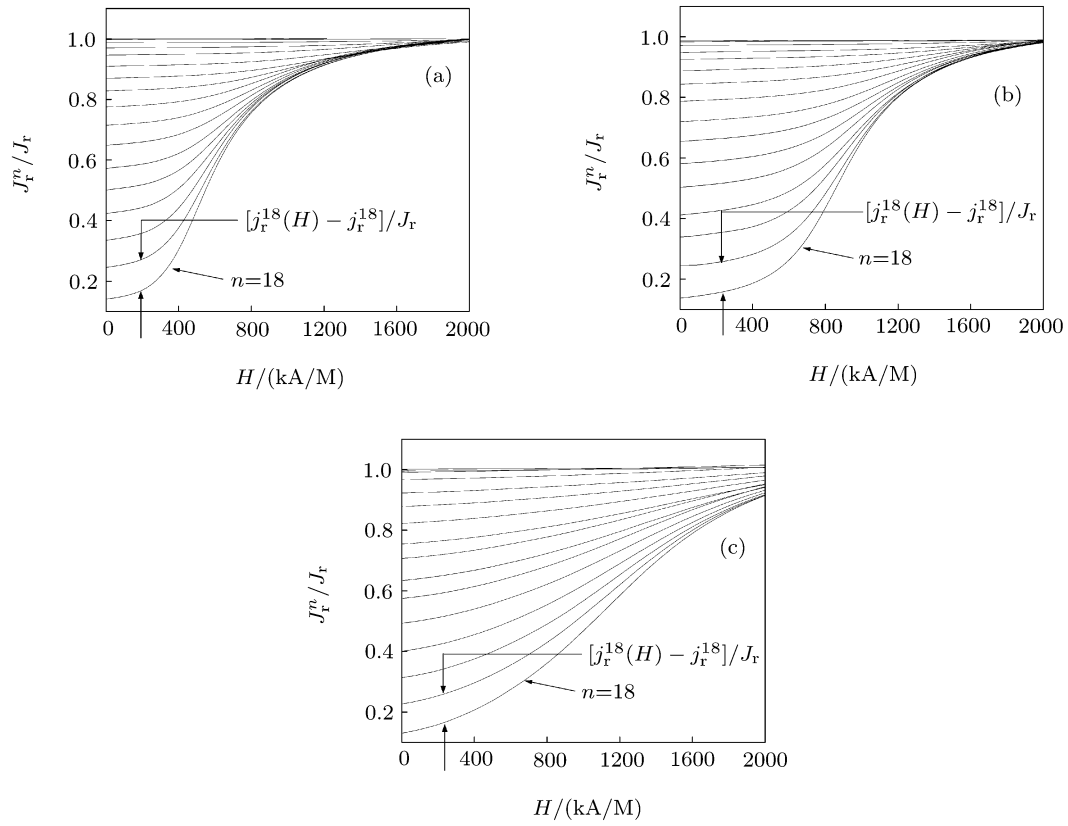


Fig.2. Set of MRC for $Pr_8Fe_{87}B_5$ (a), $Pr_{12}Fe_{82}B_6$ (b), and $Pr_{15}Fe_{77}B_8$ (c).

4. Comparison of experiment with calculations of nucleation and pinning models

Suppose Eqs.(1) and (2) are applicable to the grains of nanocrystalline magnets. According to the nucleation model or pinning model

$$j_r^n(H) = J_s \int_0^{\pi} \int_{\theta_{n-1,\phi}}^{\theta_{n,\phi}} A \sin\theta \cos\theta \mathrm{d}\theta \mathrm{d}\phi,$$

$$\begin{aligned}(A = &1 \quad \text{for} \quad H <_i H_c^{\alpha}(\theta),\\ &= -1 \quad \text{for} \quad H >_i H_c^{\alpha}(\theta). \quad \alpha = \text{n or p})\end{aligned} \tag{4}$$

where (θ, ϕ) are the polar angles of easy direction in radian unit, the integration is over whole solid angle of lamella n of initial state and $\theta_{n,\phi}$ is obtained from the relation of $\tan\theta_{n,\phi}\sin\phi = \tan\theta_n$ (Fig.3).

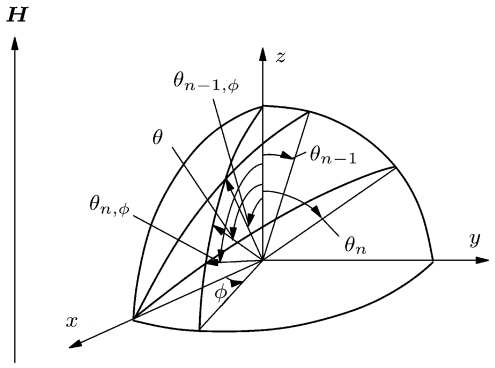


Fig.3. Geometry of θ, ϕ, $\theta_{n-1,\phi}$, θ_{n-1}, $\theta_{n,\phi}$ and θ_n in lamella n.

The integration was calculated numerically by dividing the lamella into cells of $\mathrm{d}\theta = \mathrm{d}\phi = 0.1°$. The coercivity of the lamella is the field corresponding to the maximum of the slope of the $j_\mathrm{r}^n(H)$ curve. $J_\mathrm{r}^n(H)$ is obtained from $j_\mathrm{r}^n(H)$ as

$$J_\mathrm{r}^n(H) = \sum_{\mathrm{i}}^{1,\ldots,n} [j_\mathrm{r}^i(H) - j_\mathrm{r}^i] + J_\mathrm{r}. \tag{5}$$

Figures 4(a)–4(b) show $J_\mathrm{r}^n(H/h(0))/J_\mathrm{r}$ calculated by the nucleation and pinning models.

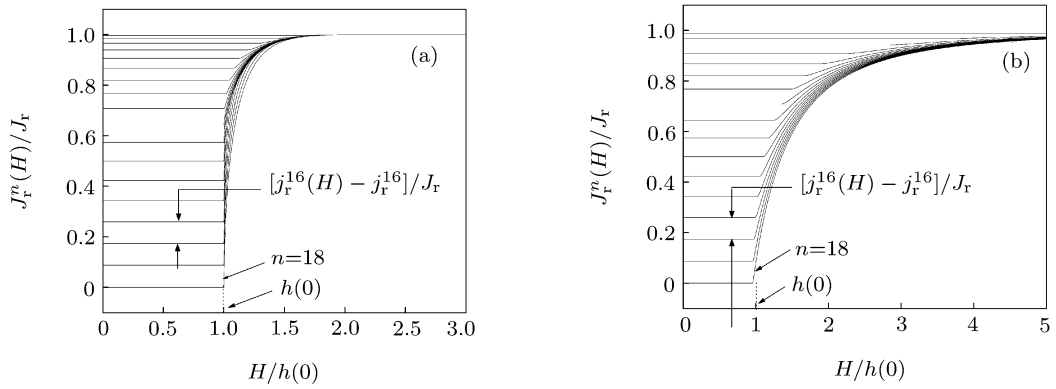


Fig.4. $J_\mathrm{r}^n(H/h(0))/J_\mathrm{s}$ calculated by the nucleation (a) and pinning (b) model.

In the above treatment it was assumed that ${}_\mathrm{i}H_\mathrm{c}^\alpha(0)$ is the same for all grains of easy axis along z-axis. It would be more reasonable to assume that they differ from each other and the distribution obeys Gaussian distribution around ${}_\mathrm{i}H_\mathrm{c}^\alpha(0)$. So the MRCs were recalculated by multiplying ${}_\mathrm{i}H_\mathrm{c}^\alpha(0)$ in the parentheses of Eq.(4) by $1 + (1/4.2)N$, where N is a real number between –4.2 and 4.2 selected randomly by procedure from a set of 50000 numbers which obey Gauss distribution $N(0,1)$. $J_\mathrm{r}^n(H/h(0))/J_\mathrm{r}$ obtained in this way are presented in Figs.5(a)–5(b), and the $h(\theta')/h(0)$ curves along with those of experiments in Figs.5(a)–5(b).

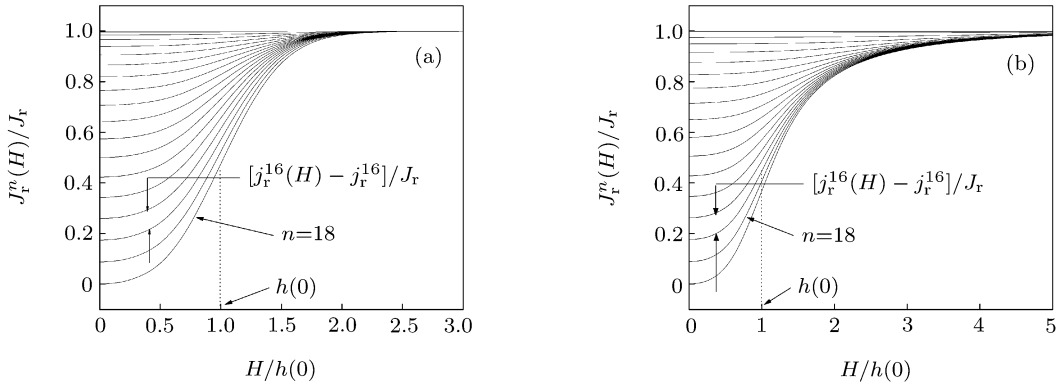


Fig.5. MRC calculated by the nucleation (a) and pinning (b) model by taking into account the Gauss distribution of ${}_\mathrm{i}H_\mathrm{c}(0)$.

5. Discussions and conclusion

$h(\theta')/h(0)$ of experiments increases monotonically with increase of θ' for all samples and simulated by the pinning model much better than the nucleation model (Fig.(6)), and hence it is concluded that the pinning of domain wall is the main mechanism of coercivity for all samples. The same conclusion has also been reached by Zhang *et al* for $Pr_2Fe_{14}B/\alpha$-Fe and $Pr_2Fe_{14}B$ ribbons.[17,18]

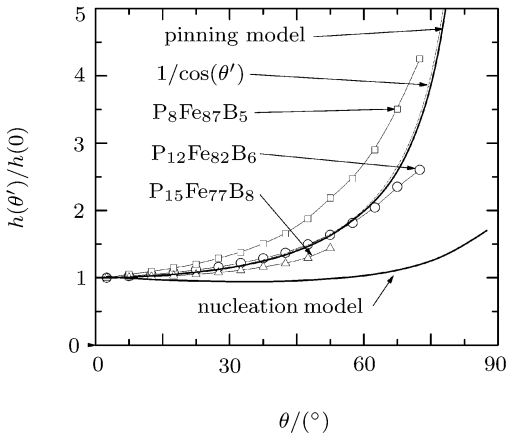


Fig.6. $h(\theta')/h(0)$ of experiments (symbols) and calculations (lines).

The increase is fastest for $Pr_8Fe_{87}B_5$ sample of smallest ${}_iH_c$ and is slowest for $Pr_{15}Fe_{77}B_8$ sample of the largest ${}_iH_c$. This is consistent with the fact that the coercivity of aligned bulk magnets of ${}_iH_c \ll H_A$ increases in proportion to $1/\cos\theta'$, but the increase is slower for the magnets of ${}_iH_c$ comparable to H_A.[19−22] Usually angular dependence of coercivity would be intermediate between that of Eq.(1) and Eq.(2) if ${}_iH_c^n(0)$ and ${}_iH_c^p(0)$ are comparable. The discrepancy of $h(\theta')/h(0)$ of small ${}_iH_c$ $Pr_8Fe_{87}B_5$ from $1/\cos\theta'$ with faster variation is not a surprise because of much complicated magnetization distribution in the nanocrystalline magnets than that of the pinning model.

References

[1] Sugana M, Fujimura S, Tagaua N, Yamomoto H and Matsuura Y 1984 *J. Appl. Phys.* **55** 2083

[2] Croat J J, Herbst J F, Lee R W and Pinkerton F E 1984 *J. Appl. Phys.* **55** 2078

[3] Buschow K H J 1991 *Rep. Prog. Phys.* **54** 1123

[4] Strnat K J In: Wohlfarth E P and Buschow K H J (ed) 1988 *Ferromagnetic Materials* **4** p131

[5] Becker J J 1976 *IEEE Trans. Magn.* **MAG-12** 965

[6] Chen R J, Zhang H W, Rong C B, Sun J R and Shen B G 2006 *J. Magn. Magn. Mater.* **305** 191

[7] Zhang H W, Zhang S Y, Shen B G, Goll D and Kronmüller H 2001 *Chin. Phys.* **10** 1169

[8] He S L, Zhang H W, Rong C B, Chen R J and Shen B G 2005 *Chin. Phys.* **14** 1055

[9] Dust K D and Kronmuller H 1987 *J. Magn. Magn. Mater.* **68** 63

[10] Pinkerton F E and Fuerst C D 1990 *J. Appl. Phys.* **67** 4735

[11] Hadjipanayis G. C, Dickenson R C and Lawless K R 1986 *J. Magn. Magn. Mater.* **54–57** 557

[12] Hadjipanayis G C, Tao Y F and Lawless K R In: 1985 Strnat K J (ed) (University of Dayton, Dayton, Ohio) *Proceedings of the Fourth International Symposium on Magnetic Anisotropy and Coercivity in Rare Earth-Transition Metal Alloys* p657

[13] Martinek G and Kronmiiller H 1990 *J. Magn. Magn. Mater.* **86** 177

[14] Givord D, Tanaud P and Viadieu T 1988 *J. Magn. Magn. Mater.* **72** 247

[15] Hermannt R, Schultzll L, Donnellv K O, Kuhtta C and Givord D 1995 *J. Phys.* D: *Appl. Phys.* **28** 2411

[16] Chen R J, Zhang H W, Rong C B, Sun J R and Shen B G 2006 *J. Appl. Phys.* **100** 9043901

[17] Zhang H W, Zhao T Y, Rong C B, Zhang S Y, Han B S and Shen B G 2003 *J. Magn. Magn. Mater.* **267** 224

[18] Zhang H W, Rong C B, Zhang J, Zhang S Y and Shen B G 2002 *Phys. Rev.* B **66** 184436

[19] Stoner E C and Wohlfarth E P 1948 *Philos. Trans. R. Soc. London* **240** 599

[20] Becker J J 1971 *AZP Conference Proceedings* 5 (New York: AIP) p1067

[21] Ratnam D V and Buessem W R 1972 *J. Appl. Phys.* **43** 1291

[22] Elbaz D, Givord D, Hirosawa S, Missell F P, Rossignol M F and Villas-Boas V 1991 *J. Appl. Phys.* **69** 5492